Chemistry–A European Journal
Research Article
doi.org/10.1002/chem.202401071
Chemistry Europe
European Chemical Societies Publishing
www.chemeurj.org

Pillar[*n*]arene-Based Fluorescence Turn-On Chemosensors for the Detection of Spermine, Spermidine, and Cadaverine in Saline Media and Biofluids

Amrutha Prabodh,[a] Laura M. Grimm,[a] Pronay Kumar Biswas,[a] Vahideh Mahram,[a] and Frank Biedermann*[a]

Polyamines are essential analytes due to their critical role in various biological processes and human health in general. Due to their role as regulators for cell growth and proliferation (putrescine and spermine), as neuroprotectors, gero-, and cardiovascular protectors (spermidine), and as bacterial growth indicators (cadaverine), rapid, simple, and cost-effective methods for polyamine detection in biofluids are in demand. The present study focuses on the development and investigation of self-assembled and fluorescent host•dye chemo-sensors based on sulfonated pillar[5]arene for the specific detection of polyamines. Binding studies, as well as stability and functionality assessments of the turn-on chemosensors for selective polyamine detection in saline and biologically relevant media, are shown. Furthermore, the practical applicability of the developed chemo-sensors is demonstrated in biofluids such as human urine and saliva.

Introduction

Biogenic polyamines, including putrescine, cadaverine, spermidine, and spermine (see Figure 1), are naturally occurring organic molecules produced through the decarboxylation of amino acids. They are prevalent in cells and body fluids of eukaryotic organisms and play a pivotal role in various biological processes.[1–5] These processes encompass essential progressions such as cell growth, proliferation, neural regulation, and immune responses.[4,6–9] Homeostasis of polyamines, in particular spermidine, has been shown to mitigate the risk of numerous cardiovascular diseases and has been recognized for its geroprotective properties.[4,10,11] Conversely, altered spermine, spermidine, and putrescine levels are associated with several severe diseases, including Alzheimer's and Parkinson's disease,[12,13] stroke,[14] heart failure,[4,11] and various cancers.[4,11,15] For example, patients suffering from the latter often exhibit elevated levels of polyamines in their urine, saliva, and blood serum.[9] Consequently, polyamines serve as valuable diagnostic markers for early-stage disease detection and monitoring of the efficacy of therapeutic interventions.[9,16–20]

Given the importance of monitoring polyamine levels, it is imperative to develop practical methods for assessing these compounds in readily accessible biofluid samples. Currently, the predominant analytical procedures for polyamine detection in biological samples are based on capillary electrophoresis and chromatographic methods, such as high-performance liquid chromatography (HPLC) and gas chromatography (GC).[21–24] While these approaches offer high precision, they come with several drawbacks, including time-consuming procedures, intricate sample pre-treatment requirements, extended analysis times, expensive equipment, and a need for specialized expertise. Hence, there is an unmatched need to develop rapid, cost-effective, and widely applicable methods for polyamine detection that offer sufficient sensitivity and selectivity.[25,26]

Fluorescence-based sensing assays have emerged as highly desirable options. These assays are characterized by their technical simplicity, affordability, real-time analyte detection capabilities, and remarkable sensitivity and selectivity. As a result, they are well-suited for high-throughput screenings (HTS).[27,28] Consequently, several reports have emerged on using fluorescent chemosensors and nanoparticle-based probes for polyamine detection.[29–36] Some notable examples include the

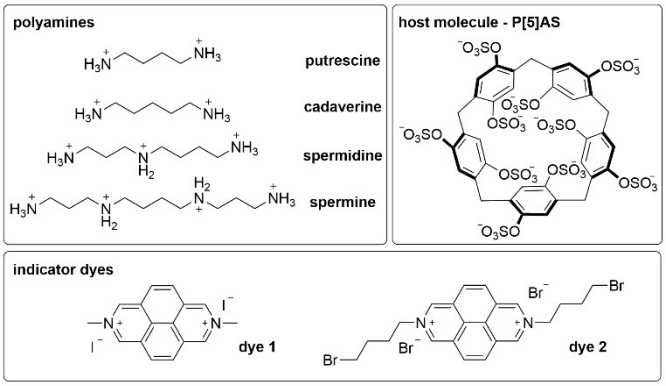

Figure 1. Chemical structures of the polyamine target analytes putrescine, cadaverine, spermidine, and spermine, the water-soluble host molecule P[5]AS, and the indicator dye molecules 1 and 2.

[a] A. Prabodh, L. M. Grimm, P. K. Biswas, V. Mahram, F. Biedermann
Institute of Nanotechnology (INT), Karlsruhe Institute of Technology (KIT), Kaiserstraße 12, 76131 Karlsruhe, Germany
E-mail: frank.biedermann@kit.edu

Supporting information for this article is available on the WWW under https://doi.org/10.1002/chem.202401071

use of negatively charged dye-embedded micelles, which exploit charge-mediated interactions to recognize polycationic polyamines, resulting in a fluorescence "turn-off" signal (see SI, Figure S1a).[29,30] Another approach involves the formation of emissive excimers by a sulfonated probe in the presence of polyamines (see SI, Figure S1b).[31] Furthermore, fluorescence-mediated host-guest interactions have been employed for polyamine detection (see SI, Figure S1c,d).[32–34] An agarose-coumarin probe deserves special mention as it can detect spermine and spermidine in aqueous buffers and spiked biofluids, albeit unphysiologically high concentrations of polyamines were required to cause the effect (see SI, Figure S1e).[36] Lastly, another interesting example involves BODIPY-functionalized gold nanoparticles (see SI, Figure S1f).[35] This approach relied on the electrostatic interactions between the negatively charged nanoparticle and the positively charged polyamines, resulting in the displacement of the cationic dye.

Despite advances, it is reasonable to conclude that the performance of most chemosensors for polyamines would likely diminish under realistic conditions. This is due to the high concentrations of salts in biofluids, which can interfere with the polyamine binding and detection mechanisms.[29–34] Furthermore, biofluids contain many organic and macromolecular components, such as amino acids, carbohydrates, other biogenic amines, proteins, and nucleobases, that can act as potential interferents. Finally, the sensitivity of reported chemosensors for polyamines in saline media does not reach the low micromolar concentration range needed for analytical applications.[29,30,32–34] Such complications underscore the need to develop and test chemosensors under realistic conditions to allow their future applications in diagnostic tests in real biofluid specimens.[33,36,37] Promising results were achieved by Cragg and coworkers, who used thiolated co-pillar[5]arene attached to the surface of a gold electrode (see SI, Figure S1g).[38] They found an analyte-selective voltammetric response to linear biogenic amines and demonstrated its applicability in biofluids. More recently, Ma and coworkers introduced a pyrene-functionalized carboxylated pillar[6]arene for the emission-based detection of spermine in live cells (see SI, Figure S1h).[39] With this contribution, we introduce two new pillar[5]arene-based (P[5]AS) fluorescent chemosensors suitable for quantitative polyamine detection in saline buffers, simulated biofluids, and spiked human urine and saliva specimens.[40]

Results and Discussion

Sulfonated pillar[*n*]arene-based molecular containers pioneered by Isaacs[41,42] are characterized by a high negative charge density packed into a small space near the portals. This functional group arrangement provides a strong electrostatic binding force for the complexation of cationic guests, which makes sulfonated pillar[*n*]arene a promising class of hosts for selective polyamine detection.[41] In addition, sulfonated pillar[*n*]arenes display a remarkably high aqueous solubility of up to 100 mM.

Herein, we explored the use of pillar[5]MaxQ (P[5]AS, see Figure 1) as a building block for a chemosensor, starting from a literature report that had investigated its strong binding affinity for polycationic compounds by ITC and NMR experiments.[41] As P[5]AS is non or only very weakly emissive and does not respond with a practically useful absorbance change upon analyte binding, our first task was to develop a chemosensing ensemble, in the following referred to as chemosensor, that is composed of P[5]AS and a suitable fluorescent dye. The chemosensor is required to maintain functionality even in saline media and biofluids and to provide a readily quantifiable fluorescence response in the presence of biogenic polyamines.

Firstly, P[5]AS was prepared from the parent hydroxylated pillar[*n*]arene, P[5]A, by reacting it with pyridine·SO_3 at 90 °C.[41] We then investigated the interaction of P[5]AS with candidate fluorescent dye molecules in aqueous solution, including in human urine (see SI, Figure S2). The tested dye molecules were berberine chloride (BC), dimethyl diazaperoperylenium dichloride (MDPP), methyl viologen dichloride (MV), lucigenin dinitrate, *trans*-4-[4-(dimethylamino)styryl]-1-methylpyridinium iodide (DSMI), 1-(adamantanyl)-4-(4-(dimethylamino)styryl)pyridinium bromide (MASAP), and dibenzyldiazapyrene dibromide (BDAP) (see SI, Figure S2b). Generally, only weak emission intensity differences were found between the dye-containing samples before and after adding P[5]AS and subsequent addition of polyamines. Consequently, such P[5]AS-dye complexes cannot be utilized as chemosensors for polyamines in biofluids and were omitted from further studies. (Likely, competitive binding of metal salt cations to the negatively charged portal regions of P[5]AS leads to host-dye disassembly in saline media and biofluids.)

Fortunately, we found a strong fluorescence quenching when combining P[5]AS with two dicationic diazapyrenium dyes, dye **1** and dye **2** in Figure 1, in deionized water, in saline aqueous media, as well as in human urine which prompted us to investigate these potential chemosensors in more detail. It is intriguing to note that diazapyrenium dyes also serve as excellent chromophores for self-assembling or constructing other biofluid-applicable chemosensors based on cucurbit[7]uril,[43–45] cucurbit[8]uril-rotaxanes,[46,47] and nanozeolites.[48]

^{1}H NMR Experiments

^{1}H NMR experiments were performed to assess whether inclusion complexes were formed between P[5]AS and the diazapyrenium dyes. We observed that the P[5]AS$^{\bullet}$**1** complex formation in D_2O is accompanied by an upfield shift and broadening of the dye proton signals (see Figure 2). This finding indicates that the dye's protons are located in the host's NMR-shielding region, as expected for an inclusion complex formed in aqueous media. Interestingly, the proton resonance signals of the host are significantly broader in the presence of **1** compared to those of the free host or the spermidine-bound host. This indicates that the flat and planar structure of pyrene-sized **1** induces a considerable deformation of the host from its

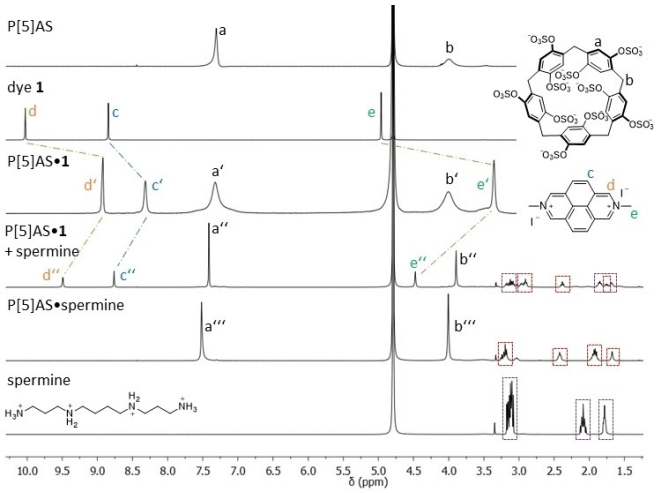

Figure 2. ^{1}H NMR spectra (500 MHz, D_2O, 298 K) recorded for P[5]AS (c = 1.0 mM), dye 1 (c = 1.0 mM), P[5]AS•1 (c = 500 μM), P[5]AS•1 mixed with spermine (equivalents 1 : 2, c(P[5]AS) = 500 μM), P[5]AS•spermine (c = 500 μM), and spermine (c = 1.0 mM).

preferred conformation. Moreover, the NMR experiments revealed that a 1 : 1 complexation stoichiometry is adopted between P[5]AS and dye **1**. The ^{1}H NMR spectra were subsequently recorded after the addition of spermine to the chemosensor solution. In the presence of 2.0 equivalent of spermine, the resonances of dye **1** shifted back towards those of the free dye while that of the host sharpened again, indicating the displacement of the dye from P[5]AS by the stronger binding analyte spermine. The small downfield shift of the host protons "a" and "b" may be caused by the deshielding effect of the polycationic charges of the encapsulated spermine guest. However, since dye **1** does not achieve the same ^{1}H NMR shifts as observed in pure D_2O, it can be inferred that residual interactions between dye **1** and the P[5]AS•spermine complex may occur, see also Figure S3 in the SI for the ^{1}H spectrum of P5[AS] and spermine in the absence of indicator dye. At the same time, several new peaks emerged in the aliphatic region that can be assigned to bound and unbound spermine that was present in stoichiometric excess. Further evidence for inclusion complex formation is provided by the NOESY cross correlations, see Figure S4 in the SI.

Absorbance and Emission Properties of 1 and 2

The photophysical properties of the self-assembled P[5]AS•**1** and P[5]AS•**2** chemosensors were investigated by UV-Vis and fluorescence spectroscopy measurements in saline phosphate buffer (1× PBS) to mimic salt concentrations typical for biofluids (see Figure 3a–c and SI, Figure S5). The indicator dyes absorb light in the near-UV to visible wavelength range with absorption bands in the 300–450 nm region. For dye **1**, the addition of P[5]AS results in an indicative 8 nm bathochromic shift of the absorbance peak maximum at 333–341 nm (see Figure 3a). Bathochromic shifts were also seen in literature reports for other pillar[*n*]arene-dye complexes,[49] and are consistent with the formation of the self-assembled P[5]AS•**1** chemosensor.

Dye **1** shows strong emission (quantum yield up to 0.63 in water)[50] in the 400–500 nm region with a maximum at 423 nm upon excitation at 436 nm (see Figure 3b). The addition of P[5]AS to **1** in 1× PBS was accompanied by a strong and almost complete quenching of the dye emission. Similarly, the addition of P[5]AS to dye **2** in 1× PBS resulted in a 4 nm bathochromic shift of the dye absorption peak maxima and was again accompanied by a strong quenching in the dye's emission (see SI, Figure S7).

Salt Effect on Binding Affinity of P[5]AS with 1 and 2.

Potential applications of the P[5]AS•dye chemosensors for molecular diagnostics applications require the stability of the self–assembled system in intricate biological fluids, such as urine, blood, and saliva containing high salt concentrations (typical concentrations for healthy human individuals are 51–190 mM Na^+ in urine[51] and 130–144 mM Na^+ in plasma[52]). Previous reports have shown that the binding affinity of many host•dye complexes significantly decreases in the presence of salts as competitive binding of metal ions to the receptor host molecule occurs.[53–56] Thus, the stability of the P[5]AS•dye chemosensors was evaluated by monitoring the binding affinity of the complexes in saline buffers with varying salt compositions such as 50 mM sodium phosphate buffer (Na-PB), 1× PBS (containing 137 mM NaCl, 2.7 mM KCl, 10 mM Na_2HPO_4, and 1.8 mM KH_2PO_4), and 10× PBS (containing 1.37 M NaCl, 27 mM KCl, 100 mM Na_2HPO_4, and 18 mM KH_2PO_4). In addition, the stability was also investigated in synthetic urine (surine), a non-biological sample whose constituents mimic human urine. A strong quenching of the dye emission was observed upon the addition of P[5]AS to either dye **1** or **2** in all media tested, including human urine (see below), indicating that the P-[5]AS•dye complexes form regardless of the salt content (see Figure 3 and SI, Figure S5–S9).

Quantitative analysis of the binding strength was then carried out through fluorescence-based titration experiments by fitting the binding isotherms to obtain the affinity (K_a) values of P[5]AS and dye **1** or **2**. High binding constants exceeding $K_a \geq 5\times10^6\ M^{-1}$ (Table 1) were found in 50 mM Na–PB, 1× PBS, and surine, suggesting that the chemosensors remain complexed and operational in micromolecular concentration ranges, as required for the detection of biogenic polyamines that occur physiologically in the micromolar concentration range. Furthermore, we tested the chemosensors' response to extreme conditions by raising the salt concentration to an unphysiologically high salt concentration of 1.37 M NaCl by using 10× PBS. Pleasingly, the P[5]AS•**1** complex formation persisted with a binding constant of $K_a = 8.7\times10^4\ M^{-1}$ even for the 10^6-times concentration excess of metal cations over dye **1** (see Figure S4c). Indicator dye **2** displayed even stronger binding to P[5]AS than indicator dye **1**. In fact, the interaction of P[5]AS and **2** in 1× PBS is so strong that the concentrations had to be

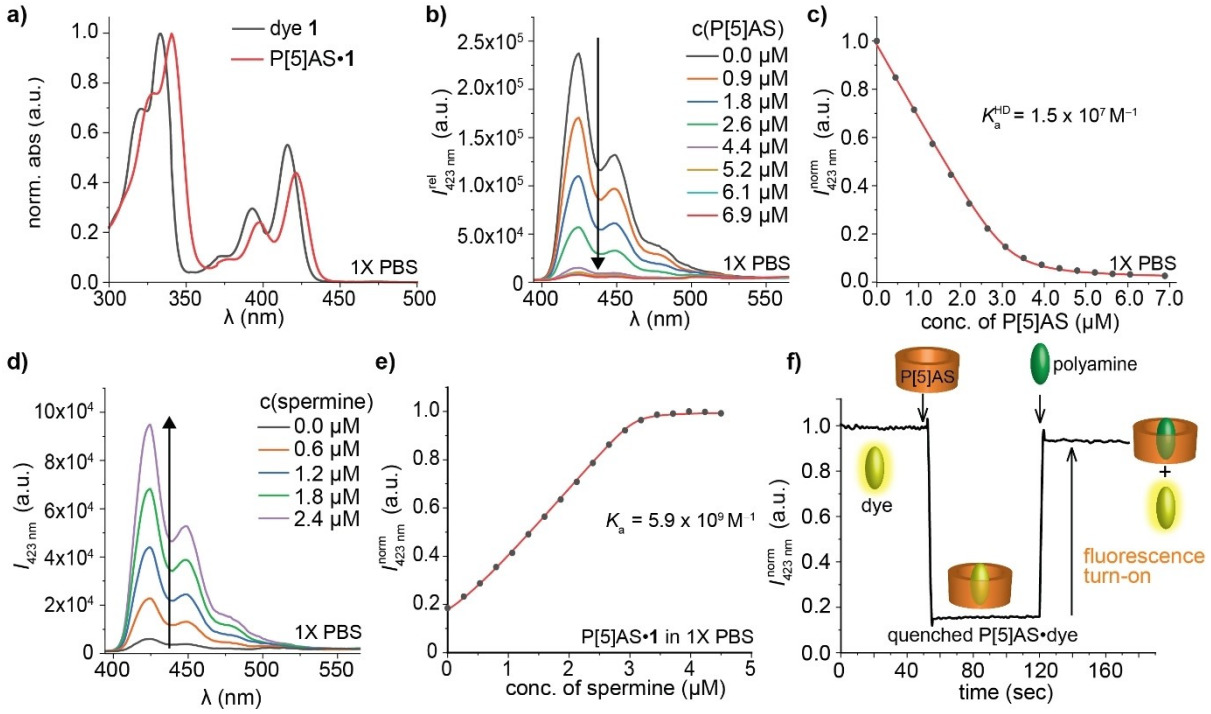

Figure 3. (a) Absorbance and (b) fluorescence emission spectra (λ_{exc} = 336 nm) of indicator dye 1 (c = 3.2 µM) upon stepwise addition of P[5]AS (c = 0–6.9 µM) in 1× PBS. (c) Normalized fluorescence emission intensity at 423 nm (λ_{exc} = 336 nm) of indicator dye 1 (c = 3.1 µM) in 1× PBS upon stepwise addition of P[5]AS (c = 0–6.9 µM). The acquired data is depicted as grey dots and the linear fitting curve as red line. The binding constant obtained is given in the graph. (d) Fluorescence emission spectra (λ_{exc} = 336 nm) of P[5]AS•1 (c = 3.1 µM) upon stepwise addition of spermidine (c = 0.0–2.4 µM) in 1× PBS. (e) Normalized fluorescence emission intensity at 423 nm (λ_{exc} = 336 nm) of P[5]AS (c = 3.1 µM) and 1 (c = 3.3 µM) upon stepwise addition of spermine (c = 0–4.6 µM). The acquired data is depicted as grey dots and the linear fitting curve as red line. The binding constant obtained is given in the graph. (f) Relative fluorescence intensity changes with time at 423 nm (λ_{exc} = 336 nm) of 1 (c = 3.1 µM) in 1× PBS upon addition of P[5]AS (c = 3.1 µM), resulting in the instantaneous formation of the emission quenched P[5]AS•1 chemosensor. The addition of the stronger binding spermine (c = 5.1 µM) results in the displacement of 1 from the host and a fluorescence signal turn-on within milliseconds.

Table 1. Experimentally determined binding affinities (K_a) for P[5]AS with indicator dyes 1 and 2, and for biogenic polyamines. The K_a values were determined by fluorescence titration experiments at 25 °C. See SI, Figure S6–S10 for the corresponding binding isotherms. Binding parameters can be found on suprabank.org (DOI: 10.34804/supra.202400313515).

Host	Dye/guest	Medium	Ka (M-1)[a]
P[5]AS	**1**	Na-PB[b]	$(4.6 \pm 0.1) \cdot 10^7$
		1× PBS	$(1.5 \pm 0.3) \cdot 10^7$
		10× PBS	$(8.7 \pm 0.1) \cdot 10^4$
		surine	$(4.9 \pm 0.4) \cdot 10^6$
P[5]AS	**2**	1× PBS	$(6.0 \pm 0.1) \cdot 10^8$
		surine	$(2.7 \pm 0.2) \cdot 10^8$
P[5]AS•**1**	spermine	Na-PB[b]	$(8.1 \pm 1.3) \cdot 10^9$
		1× PBS	$(5.9 \pm 0.5) \cdot 10^9$
		10× PBS	$(7.9 \pm 0.5) \cdot 10^5$
P[5]AS•**2**	spermine	surine	$(2.1 \pm 0.1) \cdot 10^9$
P[5]AS•**1**	spermidine	Na-PB[b]	$(1.2 \pm 0.1) \cdot 10^8$
		1× PBS	$(8.0 \pm 0.6) \cdot 10^7$
P[5]AS•**1**	cadaverine	Na-PB[b]	$(8.4 \pm 0.1) \cdot 10^7$
		1× PBS	$(4.2 \pm 0.1) \cdot 10^7$
		10× PBS	$(1.5 \pm 0.1) \cdot 10^5$

[a] Mean and standard deviation in parenthesis of at least three independent measurements, [b] 50 mM Sodium phosphate buffer, pH 7.0.

diluted to submicromolar levels to obtain a binding curve suitable for curve fitting, yielding $K_a = 6.0\times10^8\ M^{-1}$. (see SI, Figure S7a).[57,58] A competitive binding titration[59,60] with spermine as the ultra-high affinity guest for P[5]AS provided an independent and comparable estimate for the binding strength of P[5]AS•**2** as $K_a = 2.1\times10^9\ M^{-1}$ in 1× PBS (see SI, Figure S6c).

Affinity Measurements of P[5]AS with Polyamines

The host–guest binding affinity of P[5]AS with biogenic polyamines, *i.e.*, spermine, spermidine, cadaverine, and putrescine was investigated through fluorescence displacement titrations based on the competitive displacement of the indicator dye **1** or **2** from P[5]AS by the polyamine guest. Figure 3**b** displays the emission intensity monitored at 423 nm for dye **1** in 1× PBS upon the addition of P[5]AS, resulting in the in-situ formation of the P[5]AS•dye chemosensor complex, while Figure 3**d** displays the subsequent addition of spermine. The latter causes the displacement of dye **1** from P[5]AS and is accompanied by a strong fluorescence enhancement (emission turn-on sensing of polyamines), see also Figure 3e and Figure S10–S13.

The binding affinities of spermine, spermidine, and cadaverine for P[5]AS were fitted with a thermodynamic IDA model (see SI, Figure S8-S11), and the determined values are summarized in Table 1. Spermine is the strongest binder to the host P[5]AS amongst the three biogenic polyamines studied, with a binding affinity of $K_a = 5.9\times10^9\ M^{-1}$ in 1× PBS. This is followed by spermidine and cadaverine with $K_a = 8.0\times10^7\ M^{-1}$ and $K_a = 4.2\times10^7\ M^{-1}$ in 1× PBS. The binding strength of spermine, spermidine, and cadaverine to P[5]AS is sufficiently large to efficiently complex these analytes in saline aqueous media. Putrescine turned out to not displace **1** from P[5]AS, suggesting that its binding affinity for P[5]AS is much weaker than that of **1** (Figure 4a-4b). Importantly, the affinity of the P[5]AS•**2** chemosensor is so high that only micromolar concentrations of spermine but not of spermidine or cadaverine cause the dye-displacement response (see Figure 4**b**, and SI, Figure S11b). Thus, P[5]AS•**2** should be naturally capable of selectively detecting spermine, while the additional use of P[5]AS•**1** is expected to provide a quantitative response to the total concentrations of spermine, spermidine, and cadaverine.

The recorded kinetic traces suggest a rapid re-equilibration of the P[5]AS•**1** chemosensor to the addition of polyamines despite the high binding affinity of dye **1** to P[5]AS (see Figure 3f). For comparison, the guest exchange kinetic is markedly slower for the high-affinity complex of cucurbit[7]uril with dye **1**.[61] Thus, the development of a P[5]AS•**1** and P[5]AS•**2** assay for biogenic polyamine detection that is superior in assay speed compared to conventional HPLC-based polyamine detection methods[21–24] appears promising.

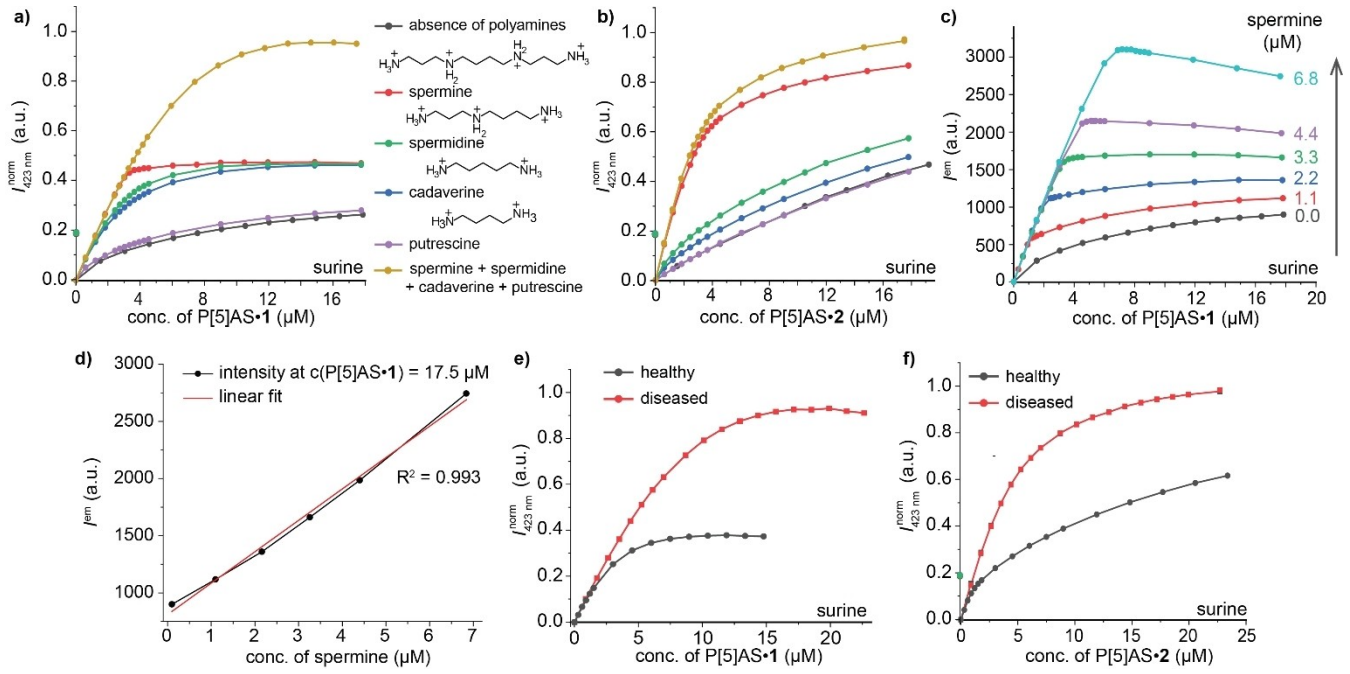

Figure 4. (a,b) Relative fluorescence emission intensity changes monitored at 423 nm upon addition of (a) P[5]AS•2 (λ_{exc} = 400 nm) and (b) P[5]AS•1 (λ_{exc} = 397 nm) to surine spiked with spermine (c = 3.3 μM, red), spermidine (c = 3.3 μM, green), cadaverine (c = 3.3 μM, blue), putrescine (c = 3.3 μM, purple), and a mixture of all four polyamines (each at c = 3.3 μM, yellow). The black line represents the fluorescence intensity of the chemosensor alone in the absence of any polyamines in surine. Data points were connected to guide the eye. (c) Relative fluorescence emission intensity changes monitored at 423 nm (λ_{exc} = 400 nm) upon addition of P[5]AS•1 chemosensor to surine with varying concentrations of spermine (c = 0–6.8 μM), resulting in distinguishable fluorescence turn-on signal outputs. (d) The connection between endpoints of data acquired in Figure 4e and concentration of added spermine enabling the creation of a calibration curve. (e)-(f) Relative fluorescence emission intensity changes at 423 nm (λ_{exc} = 397 nm) on the addition of (e) P[5]AS•1 and (f) P[5]AS•2 to surine samples with a simulated concentration of polyamines corresponding to the urine of healthy individuals (1.1 μM spermine, 1.3 μM spermidine, 2.1 μM cadaverine, and 1.9 μM putrescine) and urine of cancer patients (5.8 μM spermine, 3.2 μM spermidine, 7.8 μM cadaverine, and 7.4 μM putrescine). Data points were connected to guide the eye.

Qualitative and Quantitative Polyamine Detection in Artificial Urine

In preparation for measurements in real biofluid specimens, a chemosensor-based sensing assay was developed and tested in artificial urine (surine). Concretely, surine samples were spiked with either spermine, spermidine, cadaverine, or polyamine mixtures that physiological polyamine concentrations of human urine samples. To arrive at a practical assay that can be carried out in a microplate format, we reversed the order of compound addition from the binding affinity titration experiments, *i.e.*, a solution of the chemosensor stock solution was stepwise titrated to the analyte-containing sample, and the ensuing emission changes were monitored. In the absence of polyamines, the titration of P[5]AS•**1** to urine yielded the expected linear emission increase with increasing amount of chemosensor. These findings verify that the chemosensor complex remains fully intact even at low concentrations and that inner filter effects do not play a significant role in the chosen concentration range, as either circumstance would have led to curvature of the emission response curve. The titration of the P[5]AS•**1** chemosensor to surine spiked with individual spermine, spermidine, cadaverine, or their mixtures resulted in a much stronger and more saturation-curve-like emission increase (see Figure 4). In accordance with the results from the binding affinity titration experiments, titration of P[5]AS•**1** to a putrescine-spiked surine sample showed no significant difference compared to the control experiment with surine. In other words, putrescine does not interfere with the chemosensor-based detection and quantification of spermine, spermidine, and cadaverine.

We observed that different surine samples that were spiked with spermine in the concentration range of 1.0–6.8 μM could be readily distinguished, paving the way for developing a quantitative assay (see Figure 4**c**). Curiously, the titration of chemosensor P[5]AS•**1** to surine containing $\geq$4 μM spermine gave a triangular plot where the fluorescence intensity first linearly increases until the stoichiometric equivalence point but is then followed by a linearly decreasing intensity when higher concentrations of chemosensor are present. While the reasons for this peculiar behavior at elevated spermine concentrations are unknown to us, the reproducibly observed triangular emission response can be advantageous for determining the equivalency point and, thus, for spermine quantification (see Figure 4d).

Used on its own, P[5]AS•**1** is a chemosensor that would report on the total concentration of spermine, spermidine, and cadaverine in the media (all of which occur in the low micromolar concentration range in the urine of healthy humans). However, one can capitalize on the pronounced affinity differences between spermine and spermidine to P[5]AS to selectively detect spermine. On titration of P[5]AS•**2** to surine, a significant fluorescence turn-on was only observed for samples spiked with spermine (and its mixtures), which is consistent with the higher binding affinity of **2** than **1** for P[5]AS (see Figure 3b).

Several studies have reported elevated polyamine levels in the urine of cancer patients, which can be used as a diagnostic marker for early-stage tumor detection and to evaluate the responsiveness of patients to chemotherapy.[16,62–65] Hence, the polyamine levels in the urine of healthy individuals and cancer patients were simulated in surine based on concentration data collected from literature reports,[16,62–65] and the utility of the developed chemosensors to distinguish between healthy and diseased samples was tested. Hence, surine was spiked with 8.8 μM spermine, 10.7 μM spermidine, 17.1 μM cadaverine, and 15.5 μM putrescine to simulate polyamine concentrations levels found in the urine of healthy individuals and with 46.6 μM spermine, 25.3 μM spermidine, 62.2 μM cadaverine, and 59.5 μM putrescine to simulate critically elevated polyamine concentration levels.[16,62–65] Afterwards, the samples were diluted eight times with surine (no polyamines added) to avoid signal saturation and inner filter effects in the ensuing microplate reader-based assays. As a result, the polyamine concentrations for analysis were 1.1 μM spermine, 1.3 μM spermidine, 2.1 μM cadaverine, and 1.9 μM putrescine in surine corresponding to healthy individuals, and 5.8 μM spermine, 3.2 μM spermidine, 7.8 μM cadaverine, and 7.4 μM putrescine in surine corresponding to cancer patients. Titration of the chemosensors, P[5]AS•**1** and P[5]AS•**2**, to both the surine samples, gave clearly distinguishable fluorescence turn-on signal outputs for healthy and "diseased" urine samples (see Figure 4e-4f).

Polyamine Sensing in Neurobasal mediumtm.

Next, we evaluated the applicability of the chemosensor-based assay in neurobasal™ medium. This medium is characterized by a much higher complexity than surine and comprises of 37 different components, including amino acids, vitamins, and inorganic salts. Our choice of neurobasal™ medium for polyamine sensing studies was motivated by previous reports indicating elevated polyamine levels in the cerebrospinal fluid of individuals with human brain tumors.[66] Fortunately, the commercially available neurobasal™ medium does not contain any polyamines, so it can be used as a negative control. Hence, the medium was enriched by spiking it with spermine prior to conducting the sensing assay using the developed chemosensors. The stock solutions of the chemosensors were freshly prepared in 1× PBS and systematically titrated to the neurobasal™ medium containing spermine, leading to a fluorescence turn-on signal (see SI, Figure S13). This experimental approach served the dual purpose of validating the functionality of the chemosensors in neurobasal™ medium and establishing their capacity for selective polyamine detection. Notably, the chemosensors exhibited a remarkable capability to detect polyamines in this intricate medium without facing significant interferences from other biomolecules, including amino acids, vitamins, and salts (see SI, Figure S15). This outcome underscores the reliability and specificity of the introduced chemosensors, highlighting their potential utility in intricate biological matrices and emphasizing their effectiveness in providing selective polyamine detection in diverse physiological environments.

Polyamine Sensing in Human Urine

Having achieved promising results in surine and neurobasal medium, we extended the chemosensor assay to detect biogenic polyamines in human urine. Urinary analysis is generally receiving increasing utility in clinical diagnostics due to the availability of urine and its ease and non-invasiveness of collection.[67–70]

For our chemosensor-based polyamine detection, spot urine samples were collected from four healthy adult volunteers (the first urine of the day was omitted) and used as such without any pre-treatment or pH adjustment. Urine samples have strong absorption and fluorescence background signals arising from various metabolites present in urine[69] that absorb and emit light. To reduce the autofluorescence background of the urine samples, we diluted the urine samples two times with 1× PBS and chose an excitation wavelength where the absorbance from the urine sample was low (see SI, Figure S14).

Again, analyte spiking with spermine, spermidine, cadaverine, or their mixtures) was carried out to mimic urine samples from diseased patients,[9] *e.g.*, cancer patients, featuring elevated polyamine levels. The chemosensor assay was then conducted in a microwell plate reader format. Firstly, the autofluorescence background signal from each urine sample was recorded and used for background subtraction. Then, the fluorescence signal changes caused by adding P[5]AS•**1** or P[5]AS•**2** to the diluted urine samples were recorded.

For the chemosensor assay with P[5]AS•**1**, urine samples differing in their spermine, spermidine, and cadaverine concentration (*i.e.*, spiked vs. non-spiked) were easily distinguishable from the emission intensity readout (see Figure 5a). In contrast, selective sensing of elevated spermine levels in urine was possible using P[5]AS•**2** (see Figure 5b), as was anticipated from the results in surine.

In addition, it was possible to clearly distinguish between urine samples that are characterized by typical polyamine levels found in "healthy" and "diseased" patients.

Polyamine Sensing in Human Saliva

The application of our chemosensor-based detection for spermine, spermidine, and cadaverine was extended to human saliva analysis. Initially, a saliva sample was obtained from a healthy adult volunteer. Subsequently, various saliva samples spiked with spermine, spermidine, cadaverine, or their combinations were prepared. This approach aimed to mimic the polyamine levels typically found in the saliva of individuals with conditions like cancer.[9] The saliva sample displayed only a weak auto-fluorescence background at 423 nm when excited at 406 nm, so undiluted saliva samples were employed for the measurements. Upon the addition of P[5]AS•**1** chemosensor to the non-spiked saliva sample and to the spiked saliva samples (mimicking the medical condition of elevated polyamines), we found clearly distinguishable fluorescence emission intensities between the healthy and diseased samples (see SI, Figure S15). As for the urine assays, a distinctive fluorescence turn-on signal was only observed for saliva samples spiked with spermine when P[5]AS•**2** was used as the chemosensor. This differentiation underscores the potential of these chemosensors in selectively identifying specific polyamines in biological samples, offering a promising path for future diagnostic applications. Moreover, while we have shown the emission from the biofluid here, its autofluorescence would not be problematic in further assay development, as it can be subtracted from the signal by recording the emission intensity prior to chemosensor addition.

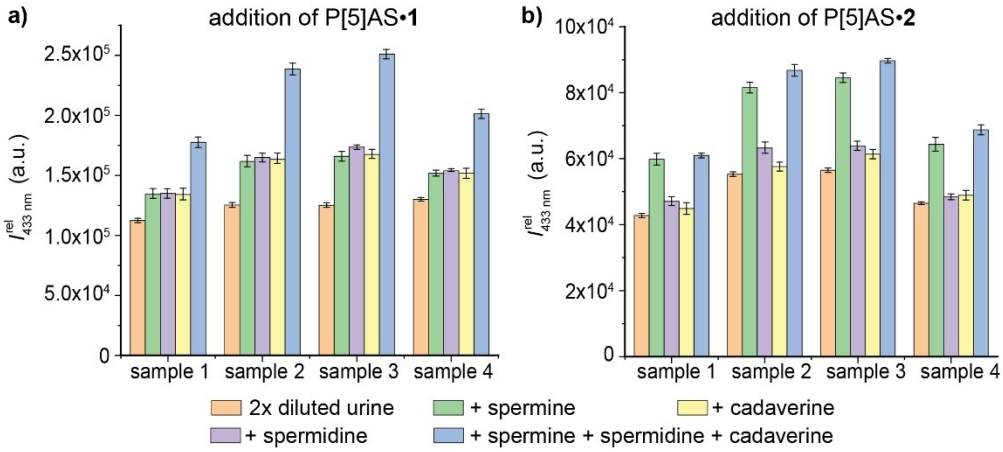

Figure 5. Relative fluorescence emission intensity changes at 433 nm (λ_{exc} = 397 nm for P[5]AS•1 and λ_{exc} = 405 nm for P[5]AS•2) upon the addition of (a) P[5]AS•1 (c = 21.6 μM) and (b) P[5]AS•2 (c = 21.6 μM) to two times diluted human urine collected from healthy individuals and later spiked with several polyamines and polyamine mixtures (each at c = 5.0 μM). The vertical error bars represent the standard deviation in the collected fluorescence emission intensity from four repetitions. The human urine fluorescence background signal was subtracted from the fluorescence signal intensity obtained following the addition of the chemosensor in all cases studied.

Conclusions

In this study, we have introduced two novel emission-based host-dye chemosensors, P[5]AS•**1** and P[5]AS•**2**, that are formed by the self-assembly of a pillar[*n*]arene-based host (P[5]AS) with highly fluorescent and strongly binding dicationic indicator dyes (**1** or **2**). These chemosensors have demonstrated exceptional suitability for the fluorescence turn-on detection of biogenic polyamines, particularly spermine, spermidine, and cadaverine, in saline buffers and various biofluids. Even in environments with high salt concentrations, their high binding affinities ensure the chemosensors' stability and applicability in biofluids. The detection mechanism of polyamines operates *via* the competitive displacement of the indicator dye by the polyamines. This mechanism, coupled with the host's high affinity for polyamines, effectively eliminates interferences from salt or other organic compounds, such as amino acids, in the sensing process. The chemosensors' functionality was validated in artificial urine (surine) and neurobasal media, and subsequently in human urine and saliva samples, showcasing their capability for selective detection of total polyamine levels by P[5]AS•**1** and specific detection of spermine by P[5]AS•**2**, with remarkable sensitivity (capable of detecting spermine concentrations as low as 1 μM). The chemosensors facilitate the differentiation between normal and elevated polyamine levels in biofluids, offering a promising avenue for early disease detection. The simplicity, cost-effectiveness, applicability for high-throughput screening, and rapid detection capabilities of these fluorescent chemosensors for polyamines underscore their potential for future development into rapid diagnostic tests suitable for home use and point-of-care settings.

Supporting Information

The authors have cited additional references within the Supporting Information.[71–73]

Acknowledgements

A.P., L.M.G., and F.B. acknowledge the Deutsche Forschungsgemeinschaft (DFG Grant BI-1805/2-1) for financial support. Open Access funding enabled and organized by Projekt DEAL.

Conflict of Interests

The authors declare no conflict of interest.

Data Availability Statement

Source data are provided with this paper and are available on zenodo with the identifier (DOI: 10.5281/zenodo.10813514). Furthermore, binding parameters and machine-readable chemical structures of the chemosensors can be found on suprabank.org (DOI: 10.34804/supra.20240313515).

Keywords: Biofluid · Fluorescence detection · Host-guest chemistry · Pillararene · Polyamine sensing

[1] E. Agostinelli, M. P. M. Marques, R. Calheiros, F. P. S. C. Gil, G. Tempera, N. Viceconte, V. Battaglia, S. Grancara and A. Toninello, *Amino Acids* **2010**, *38*, 393–403.
[2] E. Larqué, M. Sabater-Molina and S. Zamora, *Nutrition* **2007**, *23*, 87–95.
[3] K. Igarashi and K. Kashiwagi, *Int. J. Biochem. Cell Biol.* **2010**, *42*, 39–51.
[4] F. Madeo, T. Eisenberg, F. Pietrocola, G. Kroemer, *Science* **2018**, *359*, eaan2788.
[5] V. P. Singh, S. Hirose, M. Takemoto, A. M. A. S. Farrag, S.-i. Sato, T. Honjo, K. Chamoto, M. Uesugi, *J. Am. Chem. Soc.* **2024**, *146*(24), 16412–16418.
[6] A. E. Pegg, *IUBMB Life* **2009**, *61*, 880–894.
[7] S. Mandal, A. Mandal, E. J. Hans, V. O. Arturo, H. P. Myung, *Proc. Natl. Acad. Sci. USA* **2013**, *110*, 2169–2174.
[8] N. de Vera, E. Martínez, C. Sanfeliu, *J. Neurosci. Res.* **2008**, *86*, 861–872.
[9] R. A. Casero, T. Murray Stewart, A. E. Pegg, *Nat. Rev. Cancer* **2018**, *18*, 681–695.
[10] N. A. Sagar, S. Tarafdar, S. Agarwal, A. Tarafdar, S. Sharma, *Med. Sci.* **2021**, *9*, 44–65.
[11] N. Minois, D. Carmona-Gutierrez and F. Madeo, *Aging* **2011**, *3*, 716–732.
[12] L. D. Morrison and S. J. Kish, *Neurosci. Lett.* **1995**, *197*, 5–8.
[13] C. Gomes-Trolin, I. Nygren, S. M. Aquilonius, H. Askmark, *Exp. Neurol.* **2002**, *177*, 515–520.
[14] H. Tomitori, T. Usui, N. Saeki, S. Ueda, H. Kase, K. Nishimura, K. Kashiwagi, K. Igarashi, *Stroke* **2005**, *36*, 2609–2613.
[15] E. W. Gerner, F. L. Meyskens, *Nat. Rev. Cancer* **2004**, *4*, 781–792.
[16] D. H. Russell, *Nat. New Biol.* **1971**, *233*, 144–145.
[17] T. Thomas, T. J. Thomas, *J. Cell. Mol. Med.* **2003**, *7*, 113–126.
[18] C. Lo, Y.-L. Hsu, C.-N. Cheng, C.-H. Lin, H.-C. Kuo, C.-S. Huang, C.-H. Kuo, *J. Proteome Res.* **2020**, *19*, 4061–4070.
[19] Y. Asai, T. Itoi, M. Sugimoto, A. Sofuni, T. Tsuchiya, R. Tanaka, R. Tonozuka, M. Honjo, S. Mukai, M. Fujita, K. Yamamoto, Y. Matsunami, T. Kurosawa, Y. Nagakawa, M. Kaneko, S. Ota, S. Kawachi, M. Shimazu, T. Soga, M. Tomita, M. Sunamura, *Cancers* **2018**, *10*, 43–54.
[20] K. Igarashi, S. Ota, M. Kaneko, A. Hirayama, M. Enomoto, K. Katumata, M. Sugimoto, T. Soga, *J. Chromatogr. A* **2021**, *1652*, 462355.
[21] M. Y. Khuhawar and G. A. Qureshi, *J. Chromatogr. B Biomed. Appl.* **2001**, *764*, 385–407.
[22] Z. Dai, Z. Wu, J. Wang, X. Wang, S. Jia, F. W. Bazer, G. Wu, *Amino Acids* **2014**, *46*, 1557–1564.
[23] Y. Ma, G. Liu, M. Du, I. Stayton, *Electrophoresis* **2004**, *25*, 1473–1484.
[24] M. Niitsu, K. Samejima, S. Matsuzaki, K. Hamana, *J. Chromatogr. A* **1993**, *641*, 115–123.
[25] J. Krämer, R. Kang, L. M. Grimm, L. De Cola, P. Picchetti, F. Biedermann, *Chem. Rev.* **2022**, *122*, 3459–3636.
[26] S. Sinn, F. Biedermann, *Isr. J. Chem.* **2018**, *58*, 357–412.
[27] D. Wu, A. C. Sedgwick, T. Gunnlaugsson, E. U. Akkaya, J. Yoon, T. D. James, *Chem. Soc. Rev.* **2017**, *46*, 7105–7123.
[28] A. P. Demchenko, in Introduction to Fluorescence Sensing, Springer International Publishing, 2020, ch. Chapter 1–Principles and Techniques in Chemical and Biological Sensing, pp. 1–29.
[29] Z. Köstereli, K. Severin, *Chem. Commun.* **2012**, *48*, 5841–5843.
[30] J. Tu, S. Sun, Y. Xu, *Chem. Commun.* **2016**, *52*, 1040–1043.
[31] T.-I. Kim, Y. Kim, *Chem. Commun.* **2016**, *52*, 10648–10651.
[32] C. Zhong, C. Hu, R. Kumar, V. Trouillet, F. Biedermann, M. Hirtz, *ACS Appl. Nano Mater.* **2021**, *4*, 4676–4687.
[33] A. D'Urso, G. Brancatelli, N. Hickey, E. Farnetti, R. De Zorzi, C. Bonaccorso, R. Purrello, S. Geremia, *Supramol. Chem.* **2016**, *28*, 499–505.
[34] C. P. Carvalho, R. Ferreira, J. P. Da Silva, U. Pischel, *Supramol. Chem.* **2013**, *25*, 92–100.
[35] T.-I. Kim, J. Park, Y. Kim, *Chem. Eur. J.* **2011**, *17*, 11978–11982.
[36] R. R. Nair, S. Debnath, S. Das, P. Wakchaure, B. Ganguly, P. B. Chatterjee, *ACS Appl. Bio Mater.* **2019**, *2*, 2374–2387.
[37] B. Lee, R. Scopelliti, K. Severin, *Chem. Commun.* **2011**, *47*, 9639–9641.
[38] R. Reddy Kothur, B. A. Patel, P. J. Cragg, *Chem. Commun.* **2017**, *53*, 9078–9080.

[39] L. Ling, Z. Zhao, L. Mao, S. Wang and D. Ma, *Chem. Commun.* **2023**, *59*, 14161–14164.
[40] A. Prabodh, *Ph.D. Thesis* **2022**, DOI: 10.5445/ir/1000150512.
[41] W. Xue, P. Y. Zavalij, L. Isaacs, *Angew. Chem. Int. Ed.* **2020**, *59*, 13313–13319.
[42] D. King, C. R. Wilson, L. Herron, C.-L. Deng, S. Mehdi, P. Tiwary, F. Hof, L. Isaacs, *Org. Biomol. Chem.* **2022**, *20*, 7429–7438.
[43] C. Hu, L. Grimm, A. Prabodh, A. Baksi, A. Siennicka, P. A. Levkin, M. M. Kappes, F. Biedermann, *Chem. Sci.* **2020**, *11*, 11142–11153.
[44] N. M. Kumar, P. Picchetti, C. Hu, L. M. Grimm, F. Biedermann, *ACS Sens.* **2022**, *7*, 2312–2319.
[45] V. Sindelar, M. A. Cejas, F. M. Raymo, A. E. Kaifer, *New J. Chem.* **2005**, *29*, 280–282.
[46] J. Krämer, L. M. Grimm, C. Zhong, M. Hirtz, F. Biedermann, *Nat. Commun.* **2023**, *14*, 518.
[47] S. Sinn, E. Spuling, S. Bräse, F. Biedermann, *Chem. Sci.* **2019**, *10*, 6584–6593.
[48] L. M. Grimm, S. Sinn, M. Krstić, E. D'Este, I. Sonntag, E. A. Prasetyanto, T. Kuner, W. Wenzel, L. De Cola, F. Biedermann, *Adv. Mater.* **2021**, *33*, 2104614.
[49] Q. Duan, Y. Xing, K. Guo, *Front. Chem.* **2021**, *9*, 8160690.
[50] A. M. Brun, A. Harriman, *J. Am. Chem. Soc.* **1991**, *113*, 8153–8159.
[51] What Is the Chemical Composition of Urine?, https://www.thoughtco.com/the-chemical-composition-of-urine-603883, (accessed: March, 2022).
[52] H. A. Krebs, *Annu. Rev. Biochem.* **1950**, *19*, 409–430.
[53] W. Ong, A. E. Kaifer, *Org. Chem.* **2004**, *69*, 1383–1385.
[54] S. Zhang, L. Grimm, Z. Miskolczy, L. Biczók, F. Biedermann, W. M. Nau, *Chem. Commun.* **2019**, *55*, 14131–14134.
[55] V. Francisco, A. Piñeiro, W. M. Nau, L. García-Río, *Chem. Eur. J.* **2013**, *19*, 17809–17820
[56] C. Márquez, R. R. Hudgins, W. M. Nau, *J. Am. Chem. Soc.* **2004**, *126*, 5806–5816.
[57] Y. S. Day, C. L. Baird, R. L. Rich, D. G. Myszka, *Protein Sci.* **2002**, *11*, 1017–1025.
[58] M. K. Gilson, J. A. Given, B. L. Bush, J. A. McCammon, *Biophys. J.* **1997**, *72*, 1047–1069.
[59] B. T. Nguyen, E. V. Anslyn, *Coord. Chem. Rev.* **2006**, *250*, 3118–3127.
[60] A. C. Sedgwick, J. T. Brewster, T. Wu, X. Feng, S. D. Bull, X. Qian, J. L. Sessler, T. D. James, E. V. Anslyn, X. Sun, *Chem. Soc. Rev.* **2021**, *50*, 9–38.
[61] Z. Miskolczy, M. Megyesi, L. Biczók, A. Prabodh, F. Biedermann, *Chem. Eur. J.* **2020**, *26*, 7433–7441.
[62] D. H. Russell, C. C. Levy, S. C. Schimpff, I. A. Hawk, *Cancer Res.* **1971**, *31*, 1555–1558.
[63] X. Jiang, *Biomed. Chromatogr.* **1990**, *4*, 73–77.
[64] R. Liu, Y. Jia, W. Cheng, J. Ling, L. Liu, K. Bi, Q. Li, *Talanta* **2011**, *83*, 751–756.
[65] S. Antoniello, M. Auletta, P. Magri, F. Pardo, *Int. J. Biol. Markers* **1998**, *13*, 92–97.
[66] J. P. Moulinoux, V. Quemener, M. Le Calve, M. Chatel, F. Darcel, *J. Neuro-Oncol.* **1984**, *2*, 153–158.
[67] D. Ryan, K. Robards, P. D. Prenzler, M. Kendall, *Anal. Chim. Acta* **2011**, *684*, 17–29.
[68] A. Zhang, H. Sun, X. Wu, X. Wang, *Clin. Chim. Acta* **2012**, *414*, 65–69.
[69] S. Bouatra, F. Aziat, R. Mandal, A. C. Guo, M. R. Wilson, C. Knox, T. C. Bjorndahl, R. Krishnamurthy, F. Saleem, P. Liu, Z. T. Dame, J. Poelzer, J. Huynh, F. S. Yallou, N. Psychogios, E. Dong, R. Bogumil, C. Roehring, D. S. Wishart, *PLoS One* **2013**, *8*, e73076.
[70] J. Bartel, J. Krumsiek, K. Schramm, J. Adamski, C. Gieger, C. Herder, M. Carstensen, A. Peters, W. Rathmann, M. Roden, K. Strauch, K. Suhre, G. Kastenmüller, H. Prokisch, F. J. Theis, *PLoS Genet* **2015**, *11*, e1005274.
[71] M. A. Cejas and F. M. Raymo, *Langmuir* **2005**, *21*, 5795–5802.
[72] A. J. Blacker, J. Jazwinski, J.-M. Lehn, *Helv. Chim. Acta* **1987**, *70*, 1–12.
[73] A. Prabodh, D. Bauer, S. Kubik, P. Rebmann, F. G. Klärner, T. Schrader, L. Delarue Bizzini, M. Mayor, F. Biedermann, *Chem. Commun.* **2020**, *56*, 4652–4655.

Manuscript received: March 15, 2024
Version of record online: ■■, ■■

RESEARCH ARTICLE

This research delves into the critical role of fast and efficient polyamine detection utilizing self-assembled, fluorescent chemosensors based on sulfonated pillar[5]arene as host and diazapyrene indicator dyes. Polyamine-selective and spermine-selective host-guest pairs are introduced. Our results demonstrate the efficacy of the developed chemosensors in biofluids like human urine and saliva, offering promising advancements in biomedical diagnostics.

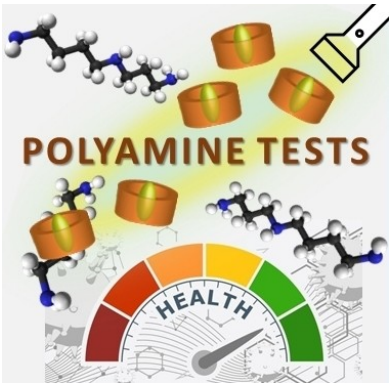

*A. Prabodh, L. M. Grimm, P. K. Biswas, V. Mahram, F. Biedermann**